ANALYSIS OF THE WORKSPACE OF CABLE-DRIVEN FORCE INTERACTIVE ROBOT

Lili LIU[1], Jihong ZUO[2*]

Based on the cable-driven parallel robot (CDPR), the feasible workspace of a cable-driven force interactive robot (CDFIR) is studied in this paper. Firstly, the structure model of the CDFIR is introduced, and the kinematics and dynamics of the CDFIR are analyzed on this basis. Secondly, the optimization model of the cable tension is given using the minimum variance optimization algorithm. The solution method and steps of the feasible workspace for the CDFIR are then given. An evaluation method of the workspace quality and the cable tension performance factor of the CDFIR are studied. Through the simulation analysis of one specific example, the influence law of the cable pre-tension force, the maximum allowable cable force, and the interaction force between the staff and the end-effector on the size of the workspace, the evaluation index of the workspace quality, and the cable tension performance factor are obtained. It provides a theoretical basis for the task planning and control method study of the CDFIR.

Keywords: cable-driven, force interactive robot, dynamics, workspace quality.

1. Introduction

The CDPRs have the characteristics of traditional rigid parallel robots and flexible cable, such as large workspace, fast motion, adjusted stiffness, simple structure, stronger reconfigurability, and good safety [1-2]. Based on the above performance advantages, the CDFIR can be used in the fields of astronaut training on the ground to simulate space operating force perception, rehabilitation training of human, sports training of the athletes, and simulation of low-gravity environment, and so on [3-4].

Combined with AR technology, the CDFIR can achieve force interactive training tasks for different application objects to improve the virtual scene training and telepresence experience of the application objects. In order to realize effective space operation training and real force perception of the application object during the training process, the robot needs to have a relatively larger working range and force feedback capability. Therefore, the size and quality of the workspace of the CDFIR is one of the important indicators for evaluating the working performance of the CDFIR [5].

The flexible cables are used as the transmission element of motion and force in the CDFIR. The cables can only provide tension force to the end-effector.

[1] Associate Professor, School of Rail Transit Intelligent Control, Hunan Railway Professional Technology College, Hunan, China, e-mail: liulili2023@outlook.com.
[2]* Lecturer, School of Rail Transit Locomotive and Rolling Stock, Hunan Railway Professional Technology College, Hunan, China, e-mail: zuojihong2006@outlook.com

Secondly, considering the safety of the operator and the robot's parameters, the cable tension should not be too large. Which requires the cable tension of the CDFIR is greater than zero and less than a certain safety value when the end-effector is at any position in the workspace. Researchers have defined the feasible workspace, the force-enclosed workspace, the force-spinning feasible workspace, and the dexterity workspace of the CDPR [6]. WANG and ZHAO et al. used Monte Carlo method to study the feasible workspace of the CDPR, and the feasible workspaces of the end-effector in different postures were analyzed [7-8]. SU and LI et al. proposed an improved Monte Carlo method. Based on the improved Monte Carlo method, the feasible workspace of the CDPR was analyzed in three cases: fixed cable length, variable cable length, and the end of the series robots and cable length are changed at the same time [9-10]. Based on the stiffness model of a CDPR, MA and SU et al. discussed the influence of cable stiffness on the workspace of the CDPR [11-12].

In the above-mentioned workspace study of the CDPRs, the influence of robot structure and other parameters on the workspace is not studied, and the distribution of robot performance in the obtained workspace is also not studied. Therefore, a CDFIR is used as the research object in this study, shown as Fig. 1. The feasible workspace of the CDFIR is analyzed based on the robot statics analysis and cable tension optimization algorithm of the CDFIR. The evaluation index of workspace quality and the cable tension distribution performance factor are then given. By changing the limit value of the cable tension and the interaction force between the worker and the end-effector, the influence of these parameters on the workspace of the CDFIR is analyzed. It lays the theoretical foundation for the task planning and cable tension planning control of the CDFIR.

2. Model of the CDFIR

2.1. Kinematic model

Fig. 1 is the structural model of the CDFIR, which is mainly composed of four cable driving units, four cables, an industrial personal computer (IPC), an end-effector and a control cabinet. The interactive force will be generated between the end-effector and the worker when the worker operates the end-effector of the CDFIR. The interactive force can be detected by the three-dimensional force sensor installed on the end-effector and uploaded to the IPC. The IPC distribute the driving torque of the four groups of cable units based on the internal algorithms. The movement of the end-effector can be realized by the coordinated motion control of the four groups of cable drive units to realize the human-machine interaction operation. The cable driving unit is composed of a motor integrated with an encoder and a force sensor and a roller wheel.

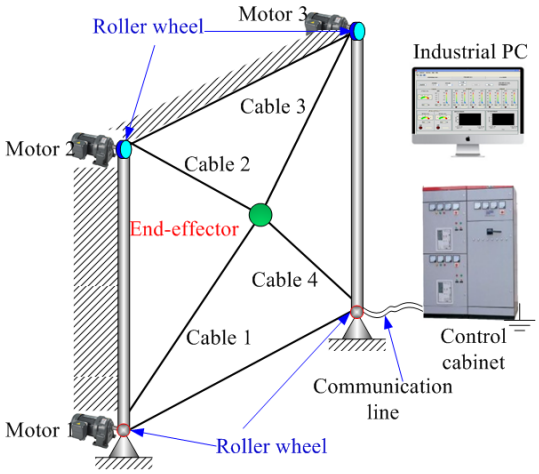

Fig. 1. The structure model of the CDFIR

The statics model of the CDFIR is shown in Fig. 2. Firstly, the global coordinate system *O-XY* is established at the center point A_1 of roller wheel 1, and the vector of the center point A_i of roller wheel i in the global coordinate system *O-XY* is denoted as $\boldsymbol{a}_i$, the vector of the origin of the end-effector O_1 in the global coordinate system *O-XY* is denoted as $\boldsymbol{b}$.

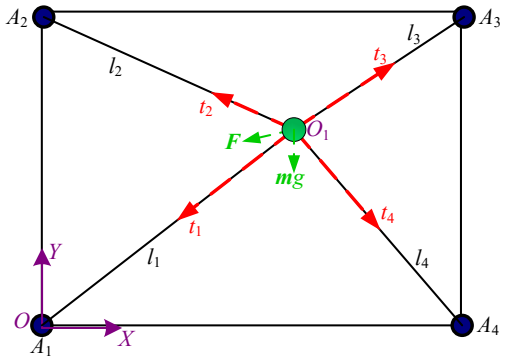

Fig. 2. The statics model of the CDFIR

Based on the vector closure principle, the length vector of the cable can be expressed as:

$$\boldsymbol{l}_i = \boldsymbol{a}_i - \boldsymbol{b},\ i = 1,2,3,4 \tag{1}$$

At this time, the unit vector of the cable can be expressed as:

$$\boldsymbol{u}_i = \boldsymbol{l}_i / l_i \tag{2}$$

2.2. Statics model

When the interaction force between the end-effector and the staff of the CDFIR is $\boldsymbol{F} = [F_x, F_y]$, the robot will drive the end-effector through four groups of cables to generate opposite force to balance the interaction force and gravity $\boldsymbol{mg}$. According to the statics balance equation, the statics model of the CDFIR can be

written as:

$$\boldsymbol{F} + m\boldsymbol{g} + \sum_{i=1}^{4} \boldsymbol{t}_i = 0 \tag{3}$$

Where $\boldsymbol{t}_i = t_i \boldsymbol{u}_i$, t_i is the tension size of the i^{th} cable.

Let $\boldsymbol{w} = -[\boldsymbol{F} + m\boldsymbol{g}]$, the statics Eq. (3) of the CDFIR can be organized as:

$$\begin{bmatrix} u_{1x} & u_{2x} & u_{3x} & u_{4x} \\ u_{1y} & u_{2y} & u_{3y} & u_{4y} \end{bmatrix} \begin{bmatrix} t_1 \\ t_2 \\ t_3 \\ t_4 \end{bmatrix} = \boldsymbol{w} \tag{4}$$

The statics model of the CDFIR can be expressed as:

$$\boldsymbol{JT} = \boldsymbol{w} \tag{5}$$

Where $\boldsymbol{J}$ is the structure matrix of the CDFIR. $\boldsymbol{T}$ is the cable tension matrix.

3. Workspace analysis

3.1. Optimization analysis of cable tensions

Because the cable can only provide one-way constraint force to the end-effector, the cable tension must be positive during actual operation. In addition, in order to further improve the stability of the CDFIR, the cable tension should have a certain pre-tensioning tension force, that is, it needs to meet the condition $t_i \geq t_{\min} > 0$. However, the maximum value of the cable force must take into account the driving characteristics of the motor and the limit value of the cable being broken. So the cable tension also needs to meet the condition $t_{\max} \geq t_i$. The cable tension meets following condition:

$$t_{\max} \geq t_i \geq t_{\min} > 0 \tag{6}$$

Where $t_{\min}$ and $t_{\max}$ denote the pre-tensioning tension and the maximum value of the cable tension, respectively.

The CDFIR contains four cables, and the end-effector has 3 degrees of freedom. The structure matrix of the CDFIR is $\boldsymbol{J} \in \boldsymbol{R}^{3\times 4}$. The rank of the structure matrix rank($\boldsymbol{J}$)=3. Therefore, the structure matrix of the CDFIR is not a square matrix, but a row full-rank matrix. It is necessary to further calculate the cable tension of the CDFIR through the generalized inverse matrix of the structure matrix $\boldsymbol{J}^{+}$:

$$\boldsymbol{T} = \boldsymbol{J}^{+}\boldsymbol{w} + Null(\boldsymbol{J})\lambda \tag{7}$$

Where $Null(\boldsymbol{J})$ denotes the zero space vector of the structure matrix. λ is an arbitrary scalar, which can be used to adjust the cable tensions.

In practical applications, the cable tension needs to be solved in real-time. Therefore, the CDFIR has higher requirements to the reasonable distribution of

cable tension, reducing the energy consumption, and quickly solve the cable tension. It is necessary to select a reasonable value λ to optimize the cable tensions. Eq. (7) can be organized as:

$$\boldsymbol{T}_{\max} - \boldsymbol{J}^{+}\boldsymbol{w} \geq Null(\boldsymbol{J})\lambda \geq \boldsymbol{T}_{\min} - \boldsymbol{J}^{+}\boldsymbol{w} \tag{8}$$

So the range of value λ is:

$$\lambda_u = \max(\min(\frac{t_{i,\min} - \left(\boldsymbol{J}^{+}\boldsymbol{w}\right)_i}{Null(\boldsymbol{J})_i}, \frac{t_{i,\max} - \left(\boldsymbol{J}^{+}\boldsymbol{w}\right)_i}{Null(\boldsymbol{J})_i})) \tag{9}$$

$$\lambda_l = \min(\max(\frac{t_{i,\min} - \left(\boldsymbol{J}^{+}\boldsymbol{w}\right)_i}{Null(\boldsymbol{J})_i}, \frac{t_{i,\max} - \left(\boldsymbol{J}^{+}\boldsymbol{w}\right)_i}{Null(\boldsymbol{J})_i})) \tag{10}$$

Where $\left(\boldsymbol{J}^{+}\boldsymbol{w}\right)_i$ denotes the special solution term of cable tension for the i^{th} cable in Eq. (5). $Null(\boldsymbol{J})_i$ denotes the zero space general solution term of cable tension for the i^{th} cable.

Therefore, the value λ should meet the following condition:

$$\lambda_u \geq \lambda \geq \lambda_l \tag{11}$$

Where λ_u and λ_l denote the upper and lower bounds of the value λ, respectively.

The CDFIR is a fully constrained mechanism. It needs to solve the cable tension value in real-time through a reasonable optimization algorithm. In order to obtain a flat and uniform distributed cable tensions, this study uses the minimum variance of the cable tensions as the optimization objective function to optimize the cable tensions. At this time, the cable tension optimization model of the CDFIR can be expressed as:

$$\begin{cases} \min\ f(\lambda) = \dfrac{1}{4}\left[\sum_{i=1}^{4}\left(t_i - \overline{t}\right)^2\right] \\ s.t.\ \ \boldsymbol{J}\boldsymbol{T} = \boldsymbol{w} \\ \quad \lambda_u \geq \lambda \geq \lambda_l \end{cases} \tag{12}$$

Where $\overline{t}$ denotes the average value of cable tensions at the current moment.

3.2. Solving algorithm of workspace

The workspace of the CDFIR is of great significance to the working performance of the robot. Specifically, it refers to the position set that the end-effector can reach when the constraint conditions of the CDFIR system are met. The mathematical description of the workspace for the CDFIR can be written as:

$$W_{\text{s}} = \{(x, y) \in \boldsymbol{R}^2 \mid f(x, y) \leq 0\} \tag{13}$$

Where W_{s} denotes the workspace for the CDFIR. $\boldsymbol{R}^2$ is a 2-dimensional real array.

Combined with the structural characteristics of the CDFIR, the position of the end-effector needs to meet the following conditions:

$$\begin{cases} \min(x_1, x_2, x_3, x_4) \le x \le \max(x_1, x_2, x_3, x_4) \\ \min(y_1, y_2, y_3, y_4) \le y \le \max(y_1, y_2, y_3, y_4) \end{cases} \tag{14}$$

Where (x_i, y_i) denotes the position of the center point A_i of roller wheel i in the global coordinate system.

The specific steps for solving the workspace of the CDFIR are as follows:

(1) Determine the structural parameters of the CDFIR and the limit value of the cable tension force according to the selected motor parameters and system stability requirements.

(2) Search for the each discrete position by determined the end-effector motion range Eq. (14). The scanning method is used to search in this study.

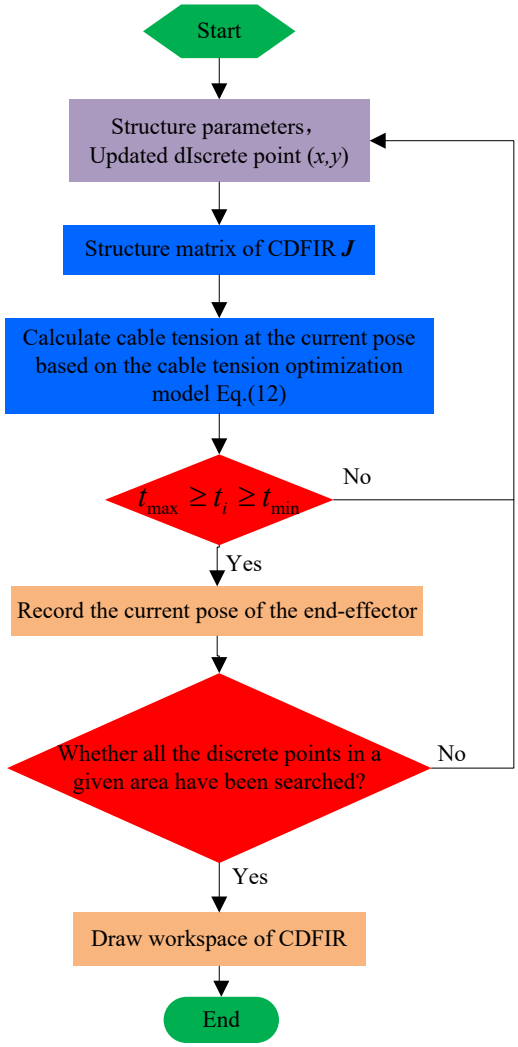

Fig. 3. The solution process of the workspace for the CDFIR

(3) By setting the external force required by the staff to complete the task, the cable tensions are calculated in the current position based on the cable tension optimization model (12). Judge whether the calculated cable tensions satisfy the Eq. (6). If it is, the current position is recorded and saved. If it is not, the current position is deleted.

(4) Repeat steps (2)-(3) until the all discrete position by determined the end-effector motion range Eq. (14) is completed. Finally, the feasible workspace of the CDFIR is drawn.

Combined with the above analysis, the solution process of the workspace for the CDFIR is shown in Fig. 3.

3.3. Evaluation of workspace quality

The workspace quality of the CDFIR can be used to measure the working performance of the robot system. Generally, the determinant of the structure matrix is used to evaluate the robot's workspace quality, but the determinant of the structure matrix has certain disadvantages in evaluating the accuracy and stability of the cable tension solution [13]. However, the condition number of the structure matrix can make up for the disadvantages of the determinant. Therefore, this study uses the condition number of the structure matrix to measure the workspace quality of the CDFIR. Therefore, the evaluation index of the workspace quality for the CDFIR can be expressed as:

$$Q = \mathrm{cond}(\boldsymbol{J}^{+}) = \sigma_{\max} / \sigma_{\min} \tag{15}$$

Where $\sigma_{\max}$ and $\sigma_{\min}$ denote the maximum singular value and the minimum singular value of the matrix $\boldsymbol{J}^{+}$, respectively, which can be obtained by performing singular value decomposition on the generalized inverse matrix of the structure matrix of the CDFIR:

$$\boldsymbol{J}^{+} = \boldsymbol{U} \sum \boldsymbol{V} \tag{16}$$

$$\sum = \begin{bmatrix} \sigma_{\max} & 0 & \cdots & 0 \\ 0 & \sigma_2 & \cdots & 0 \\ \vdots & \vdots & \ddots & \vdots \\ 0 & 0 & \cdots & \sigma_{\min} \end{bmatrix} \tag{17}$$

Where $\boldsymbol{U} \in \boldsymbol{R}^{2\times 4}$ and $\boldsymbol{V} \in \boldsymbol{R}^{2\times 2}$ are orthogonal matrices, σ_j is the singular values of matrix $\boldsymbol{J}^{+}$. The singular values satisfy the following conditions:

$$\sigma_{\max} \geq \cdots \geq \sigma_2 \geq \sigma_{\min} \geq 0 \tag{18}$$

Eq. (15) shows that the evaluation index of the workspace quality for the CDFIR is $Q \in [1, \infty)$. When Q=1, the robot system has the best kinetics transmission performance, that is, the workspace quality of the robot is the best. When $Q \to \infty$, the end-effector is in a singular position. At this time, the robot's motion mechanics transfer performance is the worst.

The workspace quality in the entire workspace of the CDFIR can be

evaluated by using the maximum value of Q in the entire workspace, that is, the evaluation index Q_w of the workspace quality of the CDFIR in the entire workspace can be expressed as:

$$Q_w = \max(\int_w Q_i) \tag{19}$$

Where Q_i denotes the condition number of the matrix $\boldsymbol{J}^+$ at different points in the workspace. $\int_w Q_i$ represents the Q of all points in the workspace. Based on the above analysis, it can be seen that when the smaller Q_w is, the better the workspace quality and the working performance of the CDFIR are.

In order to further measure the working performance of the CDFIR, this study defines the cable tension factor F_c to measure the distribution of the cable tension:

$$F_c = \frac{t_{\min}}{t_{\max}} \tag{20}$$

Where $t_{\min}$ and $t_{\max}$ denote the minimum value and the maximum value of the cable tension at current moment, respectively. When the value F_c is larger, the distribution of the cable tension is more even, and the stability of the end-effector is better.

4. Numerical example

A special case of the CDFIR is carried out for study to analyze the workspace and the workspace quality. Suppose the center point positions of the roller wheels are: A_1(0, 0)m, A_2(0, 5)m, A_3(5, 5)m, A_4(5, 0)m. The pre-tensioning force of the cables $t_{\min}$ =10N. The maximum allowable tension of the cables $t_{\max}$ =300N. The gravity of the end-effector is 100N. When the interaction force between the end-effector and the staff $\boldsymbol{F} = [F_x, F_y]$=**0**, the workspace and the evaluation index of the workspace quality for the CDFIR are shown in Fig. 4 and Fig. 5, respectively.

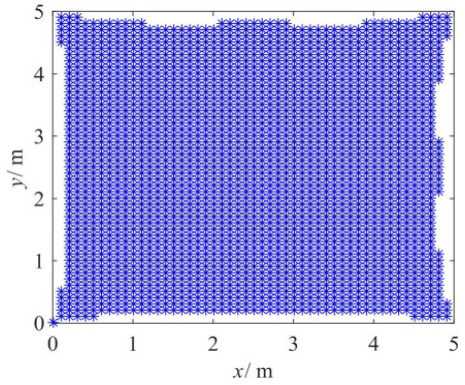

Fig.4. Workspace of the CDFIR

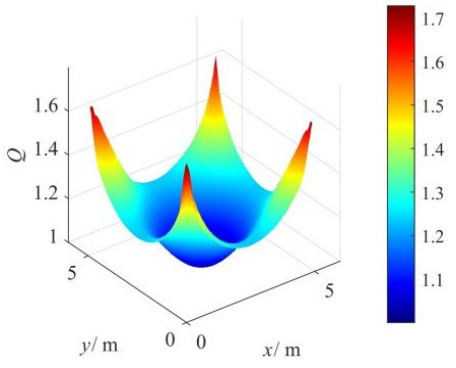

Fig.5. Workspace quality of the CDFIR

When the interaction force $\boldsymbol{F}$ =**0**, the workspace and the evaluation index of the workspace quality for the CDFIR are distributed symmetrically about the center of the workspace. At this time, the workspace of the CDFIR has 2204 discrete points. The calculation time is 1.470778s. The evaluation index of the workspace quality $Q \in [1, 1.7274]$, as shown in Fig. 5. The evaluation index of the workspace quality gradually increases from the center area of the workspace to the boundary area, which indicates that the workspace quality of the CDFIR in the central area is better than other areas, so it has good kinematics and mechanics performance in the central area. It is worth noting that the increase of value Q is obvious near the four roller wheels, and the increased amplitude is large. Therefore, the dynamical performance of the CDFIR is very poor when the end-effector is working in this area.

At this time, the distribution of F_c is shown in Fig. 6. F_c gradually decreases from the center area of the workspace to the boundary area. The larger the F_c value is, the more uniform the distribution of the cable tensions is, the better the ability to resist external interference will be, and the better the stability of the CDFIR is. The value F_c decreases rapidly at the boundary area of the workspace, which also shows that the distribution of the cable tensions at the boundary is extremely uneven, so the CDFIR has poor motion and mechanical performances. This point is consistent with the Q value result shown in Fig. 5, which indicates that the proposed evaluation index of the workspace quality is reasonable. In addition, $F_c \in [0.0546, 0.9920]$.

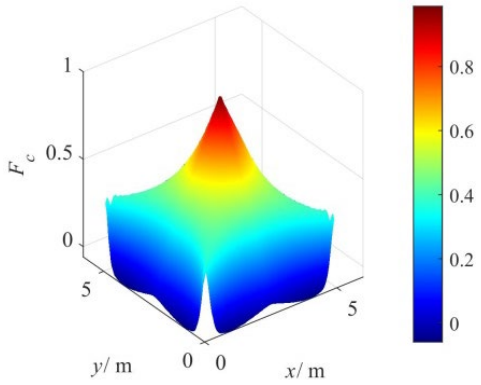

Fig. 6. Distribution of F_c

When the cable pre-tensioning force $t_{\min}$ = 30N and other parameters are the same as in Fig. 4, the workspace, the distribution of the evaluation index Q of the workspace quality and the cable tension factor F_c of the CDFIR are shown in Fig. 7.

Fig. 7 shows that when the cable pre-tensioning force is increased to $t_{\min}$ = 30N, the workspace, the distribution law of the evaluation index Q of the workspace quality and the cable tension factor F_c of the CDFIR are basically the

same with when t_{min} =10N, but the workspace is significantly reduced. The workspace has 1940 discrete points. The calculation time is 1.413146s, the calculation time is reduced. The evaluation index range of the workspace quality $Q \in [1, 1.7274]$. The range of the cable tension factor $F_c \in [0.1414, 0.9920]$, the maximum value of F_c does not change, but the minimum value of F_c increases significantly, which indicates that the increasing of t_{min} can improve the uniformity of the distribution of the cable tensions at the boundary and the ability to resist external interference. It can improve the working performance of the CDFIR.

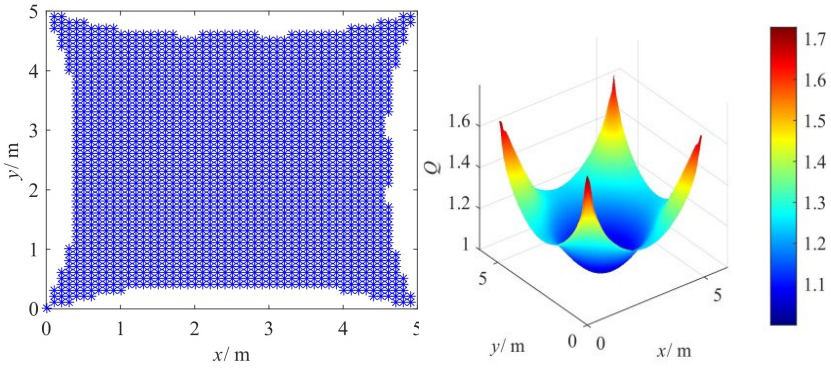

（a）Workspace of the CDFIR （b）Distribution of Q

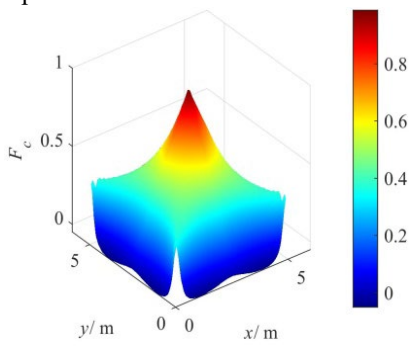

（c）Distribution of F_c

Fig. 7. Workspace, distributions of Q, and F_c of the CDFIR when t_{min} =30N

When the maximum allowable tension of the cable t_{max} =60N and other parameters are the same as in Fig. 4, the workspace, the distribution of the evaluation index Q of the workspace quality and the cable tension factor F_c of the CDFIR are shown in Fig. 8.

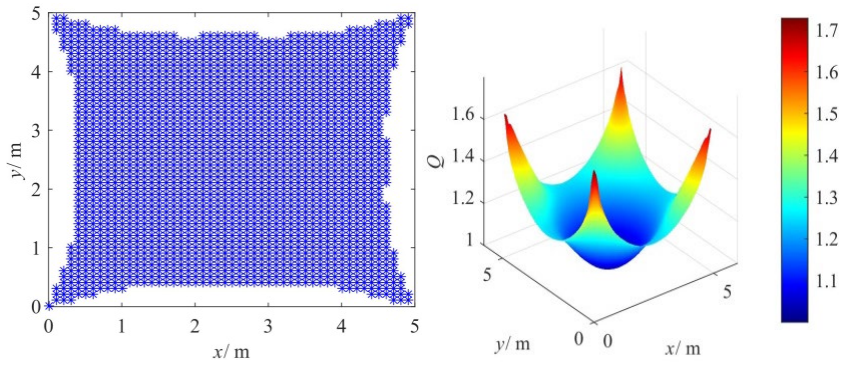

（a）Workspace of the CDFIR （b）Distribution of Q

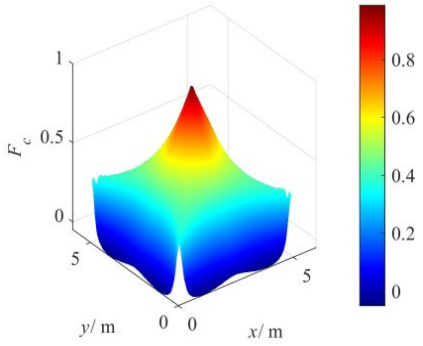

（c）Distribution of F_c

Fig. 8. Workspace, distributions of Q, and F_c of the CDFIR when $t_{\max}$ =60N

When the maximum allowable tension of the cable is reduced to $t_{\max}$ =60N, the workspace, the distribution law of the evaluation index Q of the workspace quality and the cable tension factor F_c of the CDFIR are basically the same with when $t_{\max}$ =300N, but the workspace is significantly reduced. The workspace has 1704 discrete points. The calculation time is 1.197095s, the calculation time is reduced. The evaluation index Q of the workspace quality $Q \in [1, 1.7274]$. The range of the cable tension factor $F_c \in [0.2116, 0.9920]$, the minimum value of F_c increases significantly, which indicates that the workspace of the CDFIR is reduced when $t_{\max}$ is reduced, it has almost no effect on the mechanical performance of the central area of the workspace, but has a greater impact on the working performance of the boundary area. The increase of the minimum value of F_c can improve the uniformity of the distribution of the cable tension, the performance and stability in the effective workspace of the CDFIR.

When the interaction force between the end-effector and the staff $\boldsymbol{F} = [F_x, F_y]$ =[30, 30]N and other parameters are the same as in Fig. 7, the workspace, the distribution of the evaluation index Q of the workspace quality and the cable tension factor F_c of the CDFIR are shown in Fig. 9.

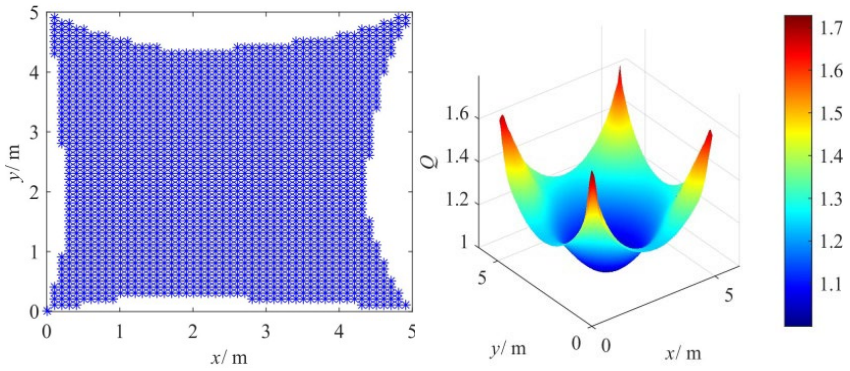

（a）Workspace of the CDFIR （b）Distribution of Q

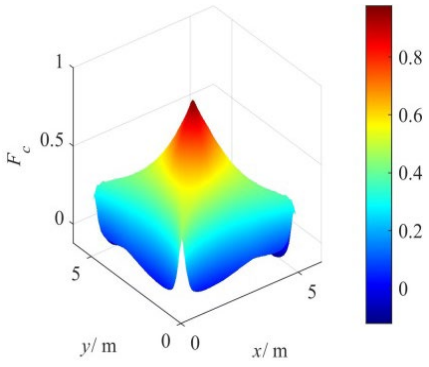

（c）Distribution of F_c

Fig. 9. Workspace, distributions of Q, and F_c of the CDFIR when $\boldsymbol{F}=[F_x, F_y]$=[30, 30]N

Fig. 9 shows that when the interaction force between the end-effector and the staff is increased to $\boldsymbol{F}=[F_x, F_y]$ =[30, 30]N, the distribution law of the evaluation index Q of the workspace quality and the cable tension factor F_c of the CDFIR are basically the same as when $\boldsymbol{F}$ =**0**N. Compared with Fig. 7, the workspace is not symmetrical about the center point (2.5, 2.5)m, and the overall workspace is significantly reduced. The workspace has 1914 discrete points. The calculation time is 1.714878s, the calculation time is increased. The evaluation index Q of the workspace quality $Q\in$[1, 1.7274]. The cable tension factor $F_c\in$ [0.1389, 0.9740], the maximum value and minimum value of F_c are significantly decreased, which indicates that the larger the interaction force $\boldsymbol{F}$ is, the smaller the workspace of the CDFIR and the calculation time are. The interaction force has a greater impact on the working performance of the boundary area. The reduction of the F_c shows that the overall working performance and stability of the CDFIR in the workspace is decreased.

In summary, when the evaluation index range of the workspace quality for the CDFIR is the same, the effective workspace of the CDFIR will be decreased with increasing the cable pre-tightening force or reducing the value of the

maximum allowable cable tension. However, the value F_c will increase in the effective workspace, which improves the overall working performance and stability of the CDFIR in the workspace. The effective workspace of the CDFIR will be decreased with increasing the interaction force between the end-effector and the staff, the value F_c will decrease in the effective workspace, which shows that the overall working performance and stability of the CDFIR in the workspace is decreased.

6. Conclusions

A CDFIR is introduced in this paper, and the problem of the kinematics, dynamics, and workspace for the CDFIR are studied.

(1) The kinematics and dynamics models of the CDFIR are established by combining the vector closure principle and mechanical equilibrium equation. The optimization of the cable tensions is discussed using the minimum variance optimization algorithm.

(2) The mathematical model of the workspace of the CDFIR is given by the combination of the structure parameters and the tension optimization model, and the evaluation index of the workspace quality and the cable tension factor are given.

(3) Through the example analysis, when the evaluation index of the workspace quality is determined, the effective workspace of the CDFIR will be decreased with increasing of the cable pre-tightening force or reducing the value of the maximum allowable cable tension. However, the overall working performance and stability of the CDFIR in the workspace is increased. The effective workspace of the CDFIR will be decreased with increasing of the interaction force between the end effector and the staff. The overall working performance and stability of the CDFIR in the workspace is also decreased. The results lay the foundation for the task planning and control strategy of the CDFIR.

Acknowledgement

This work is supported by Scientific Research Project of Department of Education of Hunan Province, China (Grant No. 20C1219). The authors wish to thank its generous financial assistance.

REFERENCES

[1] *Y. L. Wang*, *K.Y. Wang*, *K.C. Wang*, *et al. "Safety Evaluation and Experimental Study of a New Bionic Muscle Cable-Driven Lower Limb Rehabilitation Robot". Sensors, vol.20, no.24, 2020, pp.7020.*

[2] *Y. Zou*, *L. Zhang*, *L. Li*. "Force control of multimodal cable driven astronaut training robot ". Journal of Astronautics, **vol.**36, **no.**5,2015, pp.566 -573.

[3] *D. Song*, *L. Zhang*, *B.J. Wang*, *et al.* "The control strategy of Flexible Cable Driven Haptic Interactive Robot", Robot, **vol.**40, **no.**4, 2018, pp.440-447.
[4] *Y. L. Wang*, *K.Y. Wang*, *Z. X. Zhang*, *et al*. "Mechanical characteristics analysis of a bionic muscle cable-driven lower limb rehabilitation robot". Journal of Mechanics in Medicine and Biology, **vol.**20, **no.**10, 2020, pp.2040037.
[5] *L. Zhang*, *D. Song*, *L. LI*, *et al*. "Analysis of the Workspace of Flexible Cable Driven Haptic Interactive Robot", Journal of Astronautics, **vol.**39, **no.**5, 2018, pp.569-577.
[6] *Y.Q. Zheng, X.W. Liu.* "Comparison of workspace quality of 4 wire-driven parallel manipulators in 1R2T class". Journal of Mechanical Engineering， **vol.**16, **no.** 5, 2005, pp.384-389.
[7] *Y. Wang, Z. Zhao，G. Shi, et al.* "Analysis of workspace of cable-typing close-coupling multi-robot collaboratively towing system". UPB Scientific Bulletin, Series D: Mechanical Engineering, **vol**.78, **no.**4, 2016, pp.3-14.
[8] *Z. Zhao,Y. Wang,C. Su, et al.* "Analysis of the workspace and dynamic stability of a Multi-Robot Collaboratively Towing Systems". Journal of Vibration and Shock, **vol**.36， **no**.16, 2017, pp.44-50.
[9] *C. Su, J. Li, W. Ding*, *et al*. "Static workspace analysis of a multi-robot collaborative towing system with floating base". International Journal of Modeling, Simulation, and Scientific Computing, **vol**.12, **no.**2, 2021, pp. 2150009.
[10] *J. LI*, *Z.G. Zhao, S. Zhang*, et al. "Dynamics and workspace analysis of a multi-robot collaborative towing system with floating base". Journal of Mechanical Science and Technology, **vol**.35, **no.**10, 2021, pp. 4727-4735.
[11] *C. Su, J. Li, Y. Ma*, *et al*. "Motion analysis of an under-constrained multi-robots collaborative towing system based on stiffness". Scientific Bulletin Series D: Mechanical Engineering, **vol**.81, **no.** 4, 2019, pp. 5-16.
[12] *Y. Ma*, *Z.G. Zhao, Y. Wang, et al*. "Analysis of Feasible Region on the Multi Robot Combined Lifting System by Considering the Static Stiffness". Computer Simulation, **vol**.34, **no.7**, 2017, pp. 307-311+315.
[13] *Y. L. Wang, K.Y. Wang, Y.J. Chai, et al*. "Research on Mechanical Optimization Methods of Cable-Driven Lower Limb Rehabilitation Training Robot". Robotica, **vol**.40, **no.**0, 2021, pp.1-16.